THE JOURNAL OF PHYSICAL CHEMISTRY C

ARTICLE

pubs.acs.org/JPCC

A Tris-Dendrimer for Hosting Diverse Chemical Species

Pengyu Chen,[†] Yang Yang,[‡,§] Priyanka Bhattacharya,[†] Pingshan Wang,[‡] and Pu Chun Ke[†,*]

[†]Laboratory of Single-Molecule Biophysics and Polymer Physics, COMSET, [‡]Department of Electrical and Computer Engineering, Clemson University, Clemson, South Carolina 29631, United States

[§]School of Electronics and Information Engineering, Sichuan University, Chengdu, Sichuan, 610065, China

ABSTRACT: In the present experimental study, we describe the high capacity of a poly(amido amine)-tris(hydroxymethyl)amidomethane dendrimer for the physical adsorption of various chemical species (ligands), namely, cationic copper, anionic nitrate, and polyaromatic hydrocarbon phenanthrene. A pH-dependent specificity was observed for the dendrimer in hosting the chemical species, and the stoichiometric ratios of their binding were determined using UV−vis spectrophotometry. Specifically, cationic copper and anionic nitrate coordinated with the amine groups of the dendrimer through complexation and electrostatic interaction, while phenanthrene partitioned into the dendrimer interior through hydrophobic interaction. The binding and dielectric properties of the dendrimer-ligand complexes were further examined by microfluidics, at pH values optimized for the dendrimer and for species of picomolar concentrations. This study points to the vast potential of using tris-dendrimers for supramolecular assembly, environmental remediation, and nanomedicine.

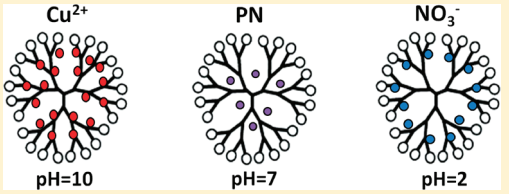

1. INTRODUCTION

Dendrimers, first envisaged by Flory[1] in 1941 and synthesized four decades later,[2−5] are polymeric architectures possessing layers or "generations" of branches emanating from a central core. Dendrimers show the most appealing characteristics such as pH-dependent contraction and swelling, amphiphilicity, ample interior voids and peripheral functional density, thermal stability, flexibility, low viscosity, and high biocompatibility.[6−9] Consequently, dendrimers have inspired active research activities over the past decades in polymer science,[6] toxicology,[10] environmental engineering,[11−13] and gene and drug delivery.[14−16] Indeed, molecular dynamics simulations[17] showed that the porous interior of poly(amido amine) (PAMAM) dendrimer affords numerous cavities for accommodating guest species. The primary and tertiary amines of the amine-terminated PAMAM dendrimer are fully protonated at pH 4 and fully neutralized at pH 10. At pH 7, the interior of the PAMAM dendrimer stays hydrophobic, while the exterior is protonated.[18] Recent studies have also shown that dendrimers such as PAMAM and poly(propylene imine) are capable of encapsulating polyaromatic hydrocarbons (PAHs),[19] inorganic solutes, and metal cations and anions and then reversibly releasing the contaminant loads upon changing the solvent pH and electrolyte strength or by a UV trigger.[12,13,20] Such binding versatility implies that dendrimers may act as a host for a variety of chemical species and serve as a "nanosponge"[19] for the remediation of contaminated water and soils.[21]

It is noted that research to date has been primarily focused on dendrimers with either $-NH_2$ or $-OH$ surface groups and for high concentrations of absorbates. For example, Diallo et al. first employed amine-terminated PAMAM dendrimers as a high capacity, recyclable, and nanoscale container for transition metal ions.[22] Zhou et al. studied the interaction between OH-terminated PAMAM dendrimer and Cu(II) using matrix-assisted laser desorption (MALDI).[23] Lard et al. demonstrated the energy transfer between phenanthrene (PN), a PAH, and a major environmental pollutant, and Alexa Fluor 350 labeled amine-terminated PAMAM dendrimer.[24] In contrast, research on the commercially available PAMAM-tris(hydroxymethyl) amidomethane dendrimer, or tris-dendrimer in short, has been surprisingly scarce. However, the trifunctional hydroxyl-surface groups and ample inner structural voids of the tris-dendrimer (Figure 1a) suggest its high capacity in hosting cationic, anionic, and hydrophobic guest species, a characteristic not readily available from any specific monofunctional NH_2 or OH-terminated PAMAM dendrimer.

Herein, we report the absorption of three chemical species—cationic copper (Cu(II)), anionic nitrate (NO_3^-), and PAH (PN) by a tris-dendrimer. The selection of these chemicals ensures the consideration of surface charge and hydrophobicity of guest species and offers a comprehensive platform for evaluating the full-range hosting capacity of the tris-dendrimer. For example, Cu(II) is a transition metal ion which readily solubilizes in water to form complexes with *d-d* transitions throughout the near-ultraviolet, visible and near-infrared regions of the spectrum. Because of its unique electronic configuration, Cu(II) is capable of forming coordination complexes with a number of polydentate ligands. On the other hand, complexation of anions is a challenging task due to their large size and high free energy of solvation. NO_3^- is a weak base that does not readily form covalent bonds with metal cations or protons. However, it interacts in a noncoordinating manner with receptors through hydrogen bonding or electrostatic

Received: March 14, 2011
Revised: June 5, 2011
Published: June 07, 2011

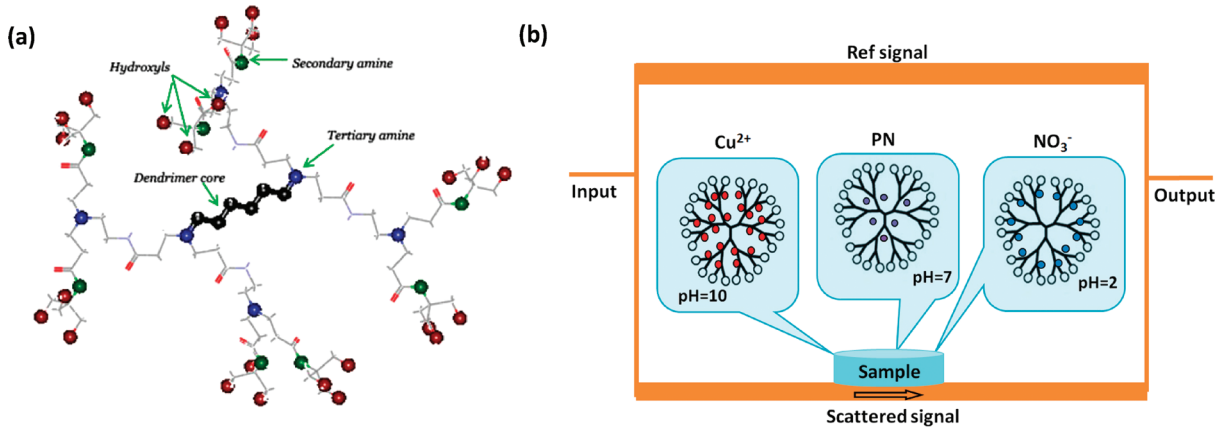

Figure 1. (a) Structure of a generation 1 tris-dendrimer, the building block of the generation 4 tris-dendrimer used in the present study. Red, oxygen; green, secondary amine; blue, tertiary amine. (b) Scheme of the microfluidic system.

interactions. Hence the receptor should be able to form several noncovalent interactions simultaneously. In addition, the selectivity of the receptor toward NO_3^- in an aqueous environment is governed by its capability to host a monoionic, trigonal planar anion as opposed to other oxoanions such as sulfate (SO_4^{2-}), phosphate (PO_4^{3-}), and hydroxyls (OH^-). In contrast to both cations and anions that have a significant solubility in water ($k_{Cu(II)}$ = 1250 g/L, $k_{NO_3^-}$ = 876 g/L),[25] PN is a PAH which is weakly soluble in water (k = 1.29 mg/L).[26] Hence, its host should be able to partition PN into a hydrophobic environment in an aqueous solution. The unique chemistry of tris-dendrimer with a highly ordered chemical structure and trifunctional groups thus, could be exceptional in hosting chemical species of varying physical properties such as mentioned above.

In the present work, specifically, the stoichiometric dendrimer–ligand ratios are determined using UV–vis spectrophotometry, and the binding mechanisms are discussed thereafter. The use of microfluidics, an engineering tool[27−31] for describing the behavior, precise control, and manipulation of fluids geometrically confined within a sub-millimeter scale, is employed to further delineate the binding and dielectric properties of the tris-dendrimer upon its binding with the chemical species at picomolar (pM) concentrations. The use of Cu(II), NO_3^-, and PN is further justified by their significant biological and environmental implications.[32−35]

2. MATERIALS AND METHODS

2.1. Materials and Characterization. Generation 4 PAMAM-tris-amidomethane dendrimer with a 1,6-diaminohexane core and 64 surface groups (MW = 18178, 10 wt % in H_2O) was purchased from Sigma Aldrich and diluted in Milli-Q (pH 6.8) to 10 μM for use. The pH values of the dendrimer solutions were adjusted to 2, 7, and 10 by titration using 1 M NaOH or HCl. The hydrodynamic sizes of the dendrimers were measured by a Nanosizer (S90, Malvern Instruments), and the surface charges of the dendrimer at the three different pH values were determined by a Zetasizer (Nano ZS, Malvern Instruments). Copper nitrate hydrate ($Cu(NO_3)_2 \cdot xH_2O$, MW = 188), sodium nitrate ($NaNO_3$, MW = 85), and phenanthrene ($C_{14}H_{10}$, MW = 178) were obtained from Sigma-Aldrich and used as the sources of Cu(II), NO_3^-, and PN, respectively.

2.2. UV–Vis Absorbance and Stoichiometric Studies of Dendrimer–Ligand Binding. To characterize the binding of the tris-dendrimer with the three chemical species, the absorbance spectra of the dendrimer-ligand complexes were measured against the control dendrimer and the chemical species using a UV–vis spectrophotometer (Biomate 3). All measurements were done using quartz cuvettes. The concentration of the dendrimer in each aqueous solution was kept constant at 10 μM while the concentrations of the species were varied. Specifically, the water-soluble Cu(II) and NO_3^- were diluted in Milli-Q, while the hydrophobic PN was dissolved in methanol. The mixtures of Cu(II), NO_3^-, and PN with the tris-dendrimer were prepared at pH 10, 2, and 7, respectively, with the molar ratio of tris-ligand kept at 1:10. The mixtures were then incubated for 30 min on a shaker prior to the measurement. Survey scans of the absorbance of the control dendrimer, the species, and the dendrimer–ligand complexes were conducted for the wavelength range of 190–800 nm. The signature peaks for the dendrimer–ligand complexes were identified. The binding dynamics of the tris-ligands were established by measuring the absorbance of the complexes at their characteristic peak wavelengths, i.e., 300 nm for tris-Cu(II), 210 nm for tris-NO_3^-, and 250 nm for tris-PN. Note the concentrations of salts added to the control tris-dendrimer and control species were the same as that added to their respective complexes to adjust the pH of the solutions.

2.3. Regeneration of Tris-Dendrimer. To investigate the recovery of tris-dendrimer on changing solution pH, the pH of the tris-ligand mixtures with the highest concentrations of species absorbed were altered by adding 1 M NaOH or 1 M HCl. The samples were then equilibrated for 30 min by constant mixing and their spectra recorded using a UV–vis spectrophotometer against the respective blanks.

2.4. Microfluidic Details. Our microfluidic device consisted of an HP8510C vector network analyzer, a Cascade probe station with ground–signal–ground (GSG) probes, and a custom-designed quartz wafer with 4-in. diameter and 500 μm in thickness.[30] The quartz wafer contained several coplanar waveguide (CPW) transmission lines and two Wilkinson power dividers. The difference in lengths between the two signal branches provided a 180° phase difference that canceled out parasitic background signals at design frequency ranges. The widths of the gap and signal lines of the CPW in the sensing zone

section were both 5 μm. The working scheme of the device is illustrated in Figure 1b. The input signal was evenly split by the Wilkinson power divider into the two branches. A signal propagating through the test branch (the bottom line) was scattered by the material in the test well which then interfered with the signal passing through the reference well on the reference branch (the top line). Denoting the path length difference between the test and the reference branches by L_1, and the physical length in the testing zone by L_2, we can calculate the phase change of the output signal as

$$\kappa_1 L_1 + (\kappa_2 - \kappa_3) L_2 \quad (1)$$

where κ_1 is the propagation constant in the transmission lines exposed to the air and κ_2 and κ_3 are the propagation constants in the test well and the reference well, respectively. Hence, when the reference well and the test well are filled with the same material, $k_2 = k_3$ and $k_1 L_1 = \pi$. This provides a 180° phase shift between the interfering signals along the two branches, resulting in a cancelation point in the frequency domain (denoted by κ_1) at which the output signal $S_{21} = 0$. When the test well is filled with a different material, the effective electrical length of the test branch is altered due to a change in permittivity in the test well.

On the basis of the principle described above, we can obtain the propagation constant in the test well (k_2) through

$$\kappa_1 L_1 + (\kappa_2 - \kappa_3) L_2 = \pi \quad (2)$$

and express the effective permittivity of the test well on the test branch as

$$\varepsilon_{\text{eff}} = \frac{{\kappa_2}^2}{4\pi^2 \varepsilon_0 \mu_0 \mu_r f^2} \quad (3)$$

where f is the frequency of cancellation point. From eq 3, we can infer that the permittivity of the sample in the test well is inversely proportional to the frequency of the cancellation point. Therefore, materials in the test well with a larger permittivity would result in a downshift of the cancellation frequency, while sample with a smaller permittivity would induce an increase of the cancellation frequency.

According to the above analysis, by incubating the dendrimer with chemical species of different concentrations, the effective permittivity of the dendrimer-ligand complex will vary due to their binding, which will be further indicated by a shift in the cancelation point of the microfluidic system.

The concentrations of the species used for microfluidic measurements ranged from 30 μM to 3 pM. The Cu(II) and NO_3^- were diluted in Milli-Q and incubated separately with the tris-dendrimer at pH 10 and 2 respectively, at a volume ratio of 1:1 for 30 min. The PN was first diluted in methanol and then incubated with the tris-dendrimer in aqueous solution at pH 7, at a volume ratio of 1:9 for 12 h. The tris-PN mixture was stored in a parafilm-covered Eppendorf tube to allow methanol evaporation, while a constant stirring was applied to the mixture to facilitate their binding. An HP8510C vector network analyzer and a Cascade probe station with GSG probes were employed to collect the scattered signals. A full two-port calibration procedure[29] was conducted prior to the measurement.

3. RESULTS AND DISCUSSION

3.1. Characterization of Tris-Dendrimer vs pH. The tris-dendrimer possessed a ζ potential of −52.9 mV at pH 10, −5.69 mV at pH 7, and 6.5 mV at pH 2, respectively. The positive charge of the dendrimer at low pH was due to the protonation of its tertiary amines and secondary amines; however, the low charge can be attributed to the shielding of positive charge by the counterions (Cl^-) in solution. The large negative charge of the dendrimer at pH 10 can be regarded due to the electron cloud dislocation as a result of the effective OH bond stretching on the terminal methyl groups, triggered by the interactions between the OH^- ions from NaOH in solution and the trihydroxyl surface groups on the dendrimer. Deprotonation of the dendrimer surface hydroxyl groups can be ruled out based on the large pK_a value of CH_3OH (pK_a = 15). The low negative charge at neutral pH may be attributed to the aforedescribed bond stretching as well. The tris-dendrimer exhibited the largest hydrodynamic size (diameter) of 4.5 nm at pH 10 compared to that of 3.1 nm at pH 2 and 2.3 nm at pH 7. Such dependence of dendrimer size on solvent pH is understandable, since the electrostatic repulsion between the three partially charged hydroxyls of each dendrimer surface group at pH 10 favored an open structure, whereas the decrease in partial charge of each dendrimer surface group compromised the electrostatic repulsion to yield a relatively hydrophobic dendrimer interior at neutral pH. At low pH, in contrast, protonation of the tertiary and secondary amines and neutralization of the surface groups promoted the dendrimer interior to become hydrophilic and the dendrimer to swell in comparison with that at neutral pH (refer to Figure 1a). A 48.8% maximum swelling at high pH was observed for the dendrimer in our experiment. This is in accordance with previous molecular dynamics simulations[36] on the pH response of charged dendrimers, where a 15% and a 50% maximum swelling were observed for the radius of gyration of the dendrimers, assuming rigid and soft bonds, respectively.

3.2. Characterization of Dendrimer−Ligand Binding with UV−Vis Spectrophotometry. The unique pH responses in the structure and net charge of the tris-dendrimer were utilized to absorb the charged and noncharged chemical species in aqueous solutions. Specifically, tris-Cu(II) and tris-NO_3^- showed characteristic broad absorbance peaks around 300 and 210 nm, respectively, whereas tris-PN displayed an increase in the PN absorbance peak at 250 nm (parts a−c of Figure 2). The appearance of characteristic peaks for tris-Cu(II) and tris-NO_3^- indicates the formation of dendrimer−ligand complexes. Specifically, Cu(II) complexed with the secondary and tertiary amine groups of the tris-dendrimer at high pH to yield a broad absorbance peak at 300 nm (290−340 nm). Such an absorbance peak is attributed to the ligand-to-metal charge transfer (LMCT)[37] between Cu(II) and the ligand groups on the tris-dendrimer. Copper in aqueous solutions exists as hexadentate $Cu(H_2O)_6^{2+}$ complexes, which undergoes ligand exchange upon interaction with the tris-dendrimer. Plausible locations of the Cu(II) are indicated in Figure 2a (right panel), following the proposed model by Ottaviani et al.[38] Coordination of Cu(II) with terminal OH groups is, however, believed to be unfeasible.[39] The band arising from LMCT was much stronger than that from the d−d transition between 600 and 800 nm (data not shown), possibly due to the low concentration (100 μM) of Cu(II) used. The low concentration of Cu(II) also did not result in the formation of copper clusters within the dendrimer. This could be inferred from the absence of the absorption peak around 570 nm that typically arises from the Mie plasmon resonance of small copper clusters.[40]

At low pH, NO_3^- formed complexes with the tertiary and secondary amine groups of the tris-dendrimer, as represented by

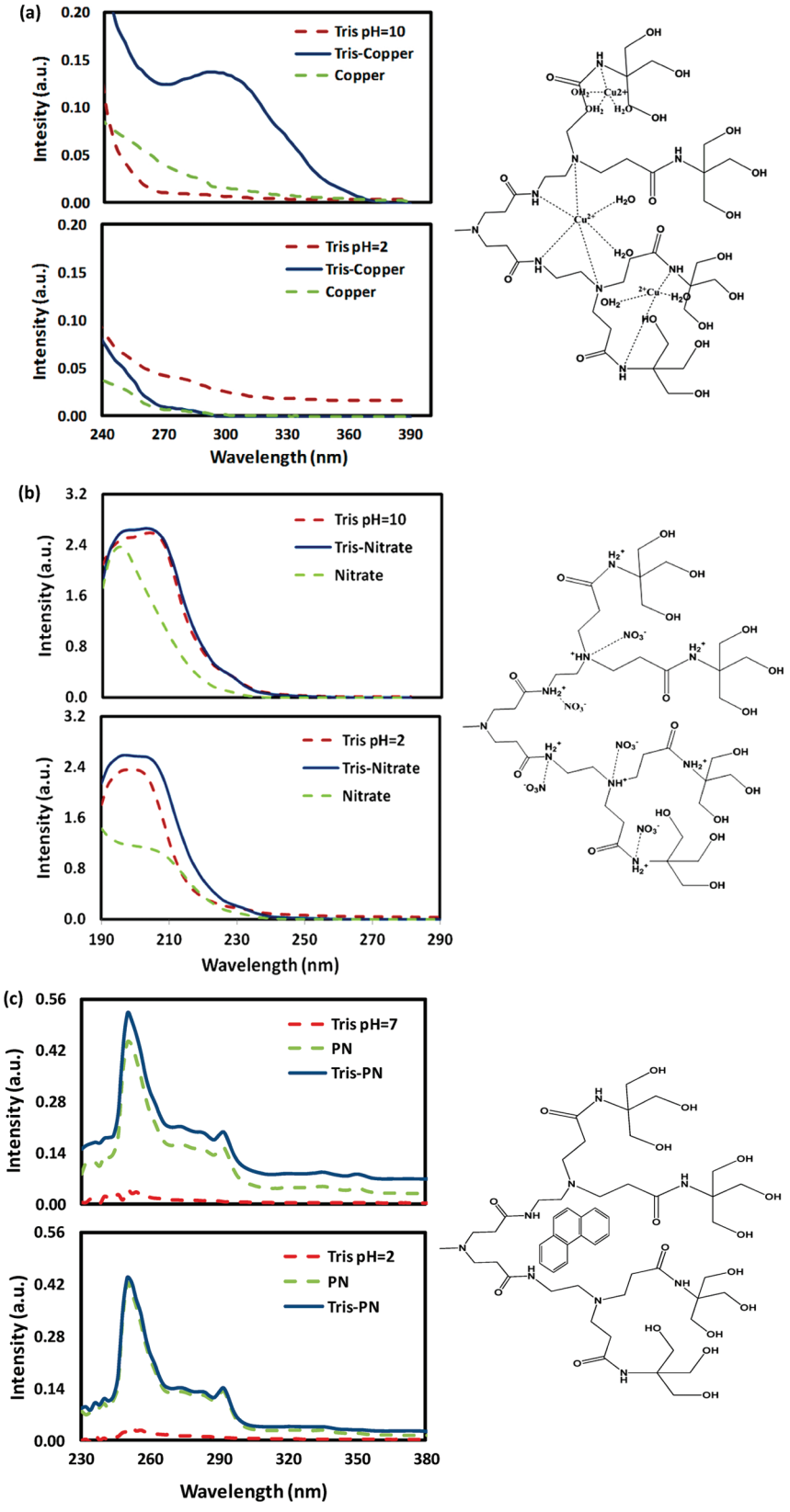

Figure 2. Absorbance spectra of (a) control tris-dendrimer, control copper, and tris-copper complex at pH 10 and 2, and enlarged branch of tris-dendrimer and possible copper coordinations at pH 10, (b) control tris-dendrimer, control nitrate, and tris-nitrate complex at pH 10 and 2, and enlarged branch of tris-dendrimer and possible nitrate coordinations at pH 2, and (c) control tris-dendrimer, control PN, and tris-PN complex at pH 7 and 2, and enlarged branch of tris-dendrimer and possible PN localization at pH 7.

dx.doi.org/10.1021/jp202417w |*J. Phys. Chem. C* 2011, 115, 12789–12796

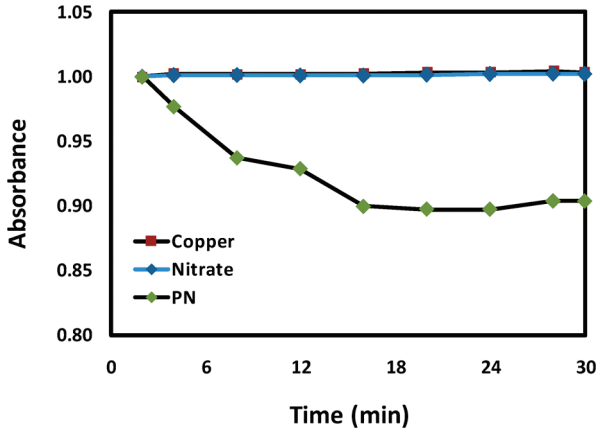

Figure 3. The binding dynamics of Cu(II), NO_3^-, and PN with tris-dendrimer. The absorbance readings were obtained at 300 nm for tris-Cu(II), 210 nm for tris- NO_3^-, and 250 nm for tris-PN, respectively, immediately following their initial incubations.

an increase in the magnitude and change in the absorbance profile of the tris-NO_3^- near 210 nm (Figure 2b). In the case of metal ions such as Cu(II), transition-metal receptors are Lewis bases that donate a pair (or pairs) of electrons to the metal via a coordinating bond. In anion coordination, the lone pair of electrons is donated in the reverse fashion from the anion to a hydrogen atom on the ligand, resulting in hydrogen-bond formation. The binding cavity then orients the H-bond in a trigonal planar coordination sphere in accordance with NO_3^- coordination.

As illustrated in Figure 2c, at neutral pH, the interaction between the PN and the tris-dendrimer is indicated by an increase of the PN absorbance peak at 250 nm, reflecting the formation of tris-PN complex from methanol to the dendrimer in the aqueous phase. It is worth noting that new absorbance bands emerged for Cu(II) and NO_3^- upon their electrostatic interactions with the tris-dendrimer. For PN, however, only an increase of the absorbance occurred resulting from its partitioning from the aqueous phase to the hydrophobic dendrimer interior. The interactions of the π-electron orbitals of the PN with the surface hydroxyl groups of the dendrimer can be ruled out due to the physisorbed waters forming H-bonds with the surface hydroxyl groups. This UV−vis measurement provided a direct evidence that tris-dendrimer can serve as a versatile host for guest species NO_3^- at low pH, PN at neutral pH, and Cu(II) at high pH. However, the projected locations of the species within the dendrimer are still speculative at this point.

The normalized binding dynamics between Cu(II), NO_3^-, and PN with the tris-dendrimer are presented in Figure 3. The binding for tris-Cu(II) and tris-NO_3^- occurred immediately after their initial mixing and remained stable over time. In comparison, the phase separation of PN started around 15 min but did not reach completion during our observation time of 48 h. This is a result of an incomplete evaporation of the methanol from solution. These dynamics further delineate the hypothesis that different binding processes took place for charged vs noncharged chemical species with the tris-dendrimer. Such contrasting binding dynamics can also be attributed to the fundamental differences between the long-range electrostatic interactions for tris-Cu(II) and tris-NO_3^- and the hydrophobic interaction for tris-PN which occurred only within the dendrimer.

To determine the maximum binding capacity of the tris-dendrimer for the chemical species, we further characterized the number of species absorbed per dendrimer through spectrophotometric titration. Parts a−c of Figure 4 indicate that each tris-dendrimer absorbed up to 64 Cu(II) ions, 32 NO_3^- ions, and 10 PN molecules, respectively. It is therefore reasonable to infer that the Cu(II) ions coordinated with the 64 secondary amine surface groups of the tris-dendrimer at high pH whereas the NO_3^- ions electrostatically bound with the 32 protonated amido groups of the dendrimer interior at low pH. Coordination of the nitrates with tertiary amines is also plausible. These observations are consistent with previous research on the binding of Cu(II) onto a generation-4 hydroxyl-terminated dendrimer.[40] However, for PN, we could approximately quantify in the following way the amount of methanol which evaporated from solution indirectly by measuring the absorbance of the control PN solution periodically. This gave us an estimated amount of PN partitioned to the air−water interface of the solution and the fraction of the partitioned PN absorbed by the tris-dendrimers. According to Beer−Lambert's law

$$[\mathrm{PN}]_n = I_{\mathrm{PN}n} \times \frac{[\mathrm{PN}]_0}{I_{\mathrm{PN}0}} \tag{4}$$

where $[\mathrm{PN}]_n$ and $[\mathrm{PN}]_0$ are the concentrations of PN in solution at time $t = n$ and 0 respectively, and I_{PN_n} and I_{PN_0} are their respective absorbance intensities. By assumption that the concentration of PN at time $t = 0$ is the total concentration of PN in solution, i.e., $[\mathrm{PN}]_0 = [\mathrm{PN}]_T$ and $\mathrm{I}_{\mathrm{PN}_0} = \mathrm{I}_{\mathrm{PN}_T}$, we have

$$[PN]_S = [PN]_T - [PN]_n \tag{5}$$

$$[\mathrm{PN}]_x = \frac{[\mathrm{PN}]_T \times I_{\mathrm{mix}n}}{I_{\mathrm{PN}T}} \tag{6}$$

where $[\mathrm{PN}]_S$ is the concentration of the PN partitioned to the air−water interface, and $[\mathrm{PN}]_x$ accounts for the concentration of the PN absorbed into the dendrimer and that is left in solution. Since the absorbance of the mixture is higher than the control PN at any time t, it is a good approximation to conclude that this extra absorbance can be attributed to the PN which has been absorbed by the tris-dendrimer from the PN partitioned to the air−water interface of the solution. Hence, the fraction of the total PN partitioned to the air−water interface of the solution absorbed by the dendrimer at the interface is given by

$$y = \frac{[\mathrm{PN}]_x - [\mathrm{PN}]_n}{[\mathrm{PN}]_S} \tag{7}$$

A plot of y vs the ratio of PN to tris-dendrimer (Figure 4c) indirectly indicates that the tris-dendrimer reaches its full capacity of capturing PN into its interior on reaching a ratio of 10:1 for PN:tris-dendrimer. At neutral pH, none or only partial surface amines of the tris-dendrimer were charged, and the neutral tris-dendrimer interior afforded a high affinity for the PN. Since hydrophobic interaction is not as specific as electrostatic interaction, the titration curve of the tris-PN complex is less smooth than that of tris-Cu(II), and tris-NO_3^-. The fluctuations in the absorbance post the saturation point (10 PN molecules to 1 tris-dendrimer, Figure 4c) further corroborate the nonspecific nature of PN partitioning within the dendrimer.

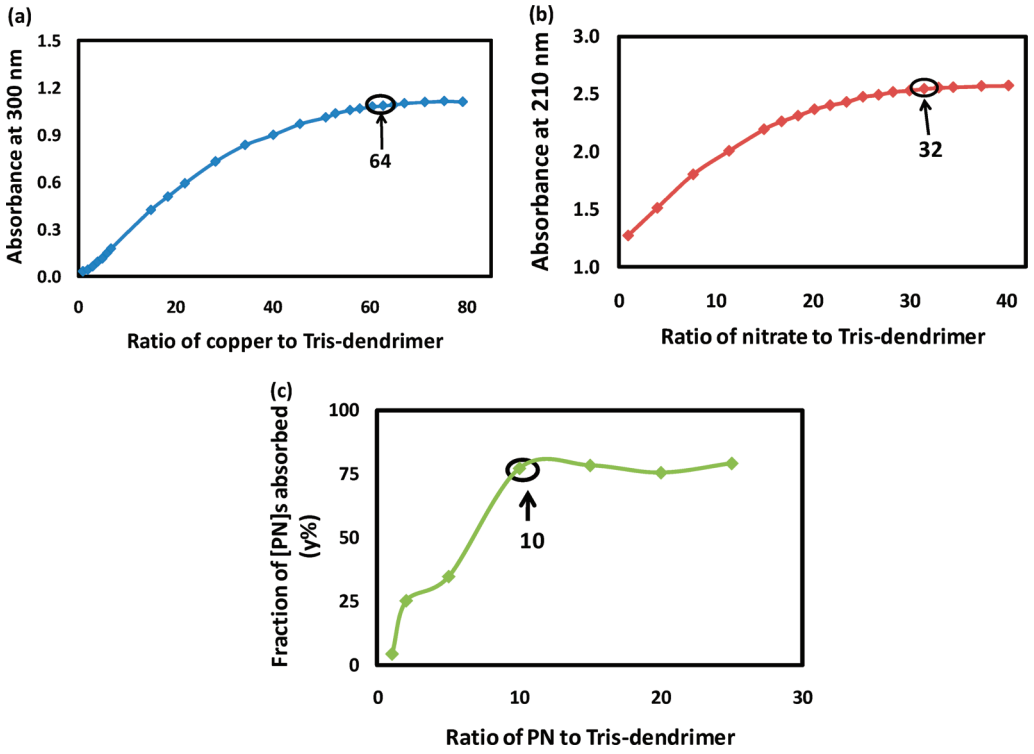

Figure 4. Spectrophotometric titration plots for (a) tris-Cu(II) at 300 nm, (b) tris-NO_3^- at 210 nm, and (c) tris-PN at 250 nm.

3.3. Dendrimer Regeneration. Binding of chemical species to the tris-dendrimer is pH dependent. Hence by simply subjecting the complexes to elevated or reduced pH, one can recover the dendrimer. As a proof of concept, on lowering the tris-Cu(II) solution pH to 2, we observed the disappearance of the complex absorbance peak (Figure 2a). At low pH, H^+ competed with Cu^{2+} for tertiary and secondary amine sites resulting in decomplexation of Cu^{2+}, and it was therefore possible to release Cu^{2+} from the dendrimer interior. Note there was a ligand exchange reaction from amines to the Cl^- (from the HCl added to lower the solution pH) and hence a formation of $CuCl_2$ was highly probable to limit hexadentate $Cu(H_20)_6^{2+}$ reformation. A similar decomplexation can be observed for NO_3^- upon increasing the tris-NO_3^- solution pH to 10, as indicated by the similarity of the complex peak and the control tris-dendrimer peak at 210 nm (Figure 2b). This resulted in a hydrophobic dendrimer interior due to tertiary and secondary amine deprotonation and repulsion of the NO_3^- from the dendrimer interior. The change in the control NO_3^- peak with pH could be attributed to the excess of NaOH at high pH and HCl at low pH, each resulting in ion association with NO_3^-.[41] It is well-known that the UV absorption spectrum of aqueous NO_3^- consists of two bands—a highly intense peak at approximately 200 nm and a much weaker peak at approximately 300 nm.[42] However, because of the low concentration of NO_3^- used in our study, the peak at 300 nm was not observed. By lowering the tris-PN solution pH to 2, the dendrimer interior became protonated, and the resulting decrease in the hydrophobicity of the dendrimer interior rejected the PN out of the dendrimer. This was indicated by a decrease in the complex peak and its resemblance to the control PN peak at low pH (Figure 2c).

3.4. Dendrimer–Ligand Binding Using Microfluidics. The aforementioned UV–vis spectrophotometry study has demonstrated the versatility of tris-dendrimer as a high-capacity chelator and host for both charged and neutral chemical species in aqueous solutions. To better understand the binding and dielectric properties of the dendrimer–ligand complexes we further conducted a microfluidic measurement of the tris-dendrimer exposed to the species of 30 μM to 3 pM in concentration. Figure 5 exemplifies the microfluidic result of the dendrimer incubated with different concentrations of NO_3^- at pH 2. The rightmost black curve indicates the control solution of the tris-dendrimer alone. With the increased concentration of NO_3^-, the cancelation points (minimum peak positions) in the frequency domain continuously shifted to the left; the peak shift was easily detectable even for a low nitrate concentration of 3 pM. If the sample in the test well possesses a higher permittivity than the control in the

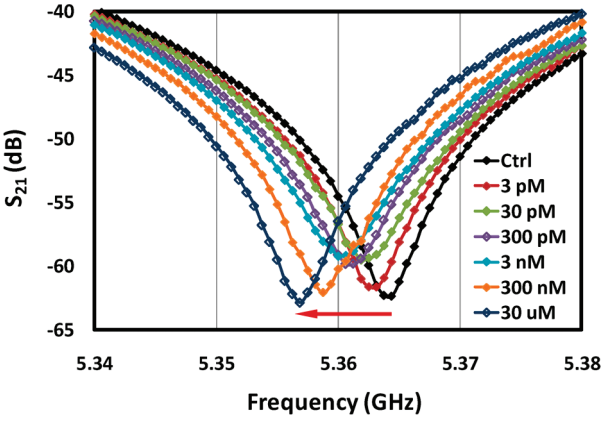

Figure 5. Exemplified microfluidic measurement of tris-nitrate binding. The tris-dendrimer at pH 2 was incubated with nitrate of 3 pM to 30 μM. An evident frequency downshift occurred with increased nitrate concentration (indicated by the red arrow).

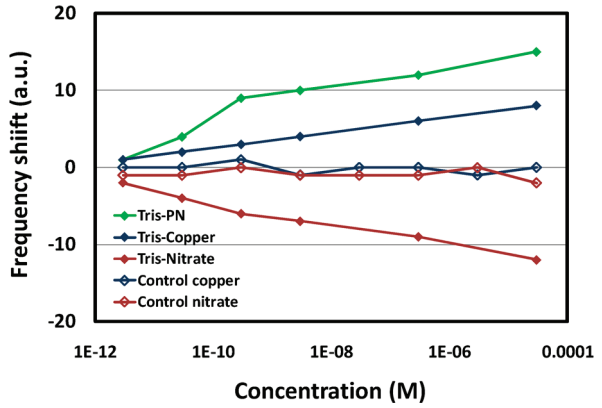

Figure 6. Frequency shifts of the tris-ligand complexes (solid diamonds) vs the controls for copper and nitrate (hollow diamonds) measured by microfluidics. The frequency shift for tris-PN was calculated by comparing the signals for tris-PN (scattered) and tris-dendrimer (reference). No PN control was available since the PN was first dissolved in methanol prior to its mixing with the dendrimer.

reference well, the effective electrical length of the test branch will increase accordingly. This will give rise to a greater difference in the effective electrical length between the test branch and the reference branch, and further trigger a downshift of the cancelation frequency to satisfy the 180° phase cancelation condition for the two branches. On the contrary, a sample of lower permittivity would cause the cancelation position to shift to a higher frequency. In the case of tris-nitrate binding, specifically, the downshifts of the cancelation position with increased nitrate concentration signified an increased tris-dendrimer permittivity due to the increased nitrate binding.

Additional microfluidic measurements were conducted for Cu(II) and PN and the results are collectively shown in Figure 6. The curves with hollow diamond markers represent the frequency shifts of the control Cu(II) and NO_3^-. No PN control was available since the PN was first dissolved in methanol prior to its mixing with the dendrimer. Interestingly, unlike the anionic NO_3^- which increased the dendrimer permittivity upon their binding (i.e., a decrease in the cancelation frequency) at pH 2, the dendrimer bound with the cationic Cu(II) or neutral PN exhibited a reduced permittivity (i.e., an increase in the cancelation frequency). Such variations in the dendrimer permittivity can be attributed to the altered dipole moment of the tris-dendrimer upon its binding with the species. Specifically, the hydroxyl and amino surface groups of the tris-dendrimer afforded the molecule charge polarities or a dipole moment. When the anionic nitrate ions were bound to the tris-dendrimer they strengthened the negative polarity of the dendrimer to yield a larger dipole moment. Higher concentrations of the nitrate ions further increased the dipole moment as well as the permittivity of the dendrimer. On the contrary, when the cationic copper ions were bound to the dendrimer, the dipole moment of the dendrimer was weakened due to the partial neutralization of the hydroxyls on the dendrimer surface. Consequently, the dendrimer−copper complex assumed a reduced permittivity with increased copper concentration. As for the PN, its complexation with the hydrophobic dendrimer interior was polarized by the external electric field applied to the microfluidic system, which compromised the dipole moment of the tris-PN complex to induce an increased cancelation frequency.

4. CONCLUSIONS

In conclusion, we have demonstrated the hosting and releasing capacity of the tris-dendrimer for various chemical species. The selective absorption and maximum loading of the tris-dendrimer have been characterized using UV−vis spectrophotometry for major chemical species of environmental relevance—copper, nitrate, and PN at different pH values. Microfluidics offered more detailed information regarding the dielectric properties and complexation of tris-dendrimer with the chemical species for chemical concentrations down to the pM level. The formation and dynamics of the dendrimer−chemical complexes have been discussed from the standpoints of physical chemistry and the electric dipole moments of the complexes in an external electric field. This study indicates that tris-dendrimer can serve as a full-range host for the adsorption and dispersion of cationic, anionic, and PAH species. The trifunctionality of the tris-dendrimer could be advantageous owing to its higher surface charge density than the cationic or anionic monofunctional PAMAM dendrimers. In addition to environmental implications such as water purification and spilled oil dispersion, the tris-dendrimer may find new applications in supramolecular chemistry, soft matter, chemical engineering, and nanomedicine.

AUTHOR INFORMATION

Corresponding Author

*E-mail: pcke11@clemson.edu. Phone: 8646560558. Fax: 8646560805.

ACKNOWLEDGMENT

Ke acknowledges the support of an NSF CAREER Award No. CBET-0744040 and US EPA Grant No. R834092. Wang acknowledges NSF Grant No. 0925424. Part of the RF sensor was fabricated at the Oak Ridge National Lab (ORNL). The authors thank Dr. Thompson Mefford for the use of a Zetasizer.

REFERENCES

(1) Flory, P. J. *J. Am. Chem. Soc.* **1941**, *63*, 3083.
(2) Denkewalter, R. G.; Kole, J.; Lukasavage, W. J. U.S. patent 4,289,872, (1981).
(3) Tomalia, D. A.; Baker, H.; Dewald, J.; Hall, M.; Kallos, G.; Martin, S.; Roeck, J.; Ryder, J.; Smith, P. *Polym. J.* **1985**, *17*, 117.
(4) Newkome, G. R.; Yao, Z. Q.; Baker, G. R.; Gupta, V. K. *J. Org. Chem.* **1985**, *50*, 2003.
(5) Hawker, C. J.; Frechet, J. M. J. *J. Am. Chem. Soc.* **1990**, *112*, 7638.
(6) Helms, B.; Meijer, E. W. *Science* **2006**, *313*, 929.
(7) Bosman, A. W.; Janssen, H. M.; Meijer, E. W. *Chem. Rev.* **1999**, *99*, 1665.
(8) Freedman, K. O.; Lee, J.; Li, Y.; Luo, D.; Skobeleva, V. B.; Ke, P. C. *J. Phys. Chem. B* **2005**, *109*, 9839.
(9) Mortimer, M.; Kasemets, K.; Heinlaan, M.; Kurvet, I.; Kahru, A. *Toxicol. Vitro* **2008**, *22*, 1412.
(10) Malik, N.; Wiwattanapatapee, R.; Klopsch, R.; Lorenz, K.; Frey, H.; Weener, J. W.; Meijer, E. W.; Paulus, W.; Duncan, R. *J. Controlled Release* **2000**, *65*, 133.
(11) Diallo, M. S.; Christie, S.; Swaminathan, P.; Johnson, J. H., Jr.; Goddard, W. A., III. *Environ. Sci. Technol.* **2005**, *39*, 1366.
(12) Diallo, M. S.; Falconer, K.; Johnson, J. H., Jr; Goddard, W. A., III. *Environ. Sci. Technol.* **2007**, *41*, 6521.
(13) Diallo, M. S.; Arasho, W.; Johnson, J. H., Jr.; Goddard, W. A., III. *Environ. Sci. Technol.* **2008**, *42*, 1572.
(14) Malik, N.; Duncan, R.; Tomalia, D. A.; Esfand, R. U.S. patent 7,005,124, (2006).

(15) Haensler, J; Szoka., F. C., Jr. *Bioconjugate Chem.* **1993**, *4*, 372.
(16) Tang, M. X.; Redemann, C. T.; Szoka, F. C., Jr. *Bioconjugate Chem.* **1996**, *7*, 703.
(17) Maiti, P. K.; Cagin, T.; Wang, G.; Goddard, W. A., III. *Macromolecules* **2004**, *37*, 6236.
(18) Maiti, P. K.; Cagin, T.; Lin, S.; Goddard, W. A., III. *Macromolecules* **2005**, *38*, 979.
(19) Arkas, M.; Tsiourvas, D.; Paleos, C. M. *Chem. Mater.* **2003**, *15*, 2844.
(20) Meijer, E. W.; van Genderen, M. H. P. *Nature* **2003**, *426*, 128.
(21) Xu, Y.; Zhao, D. *Ind. Eng. Chem. Res.* **2006**, *45*, 1758.
(22) Diallo, M. S.; Balogh, L.; Shafagati, A.; Johnson, J. H.; Goddard, W. A., III.; Tomalia, D. A. *Environ. Sci. Technol.* **1999**, *33*, 820.
(23) Zhou, L.; Russell, D. H.; Zhao, M.; Crooks, R. M. *Macromolecules* **2001**, *34*, 3567.
(24) Lard, M.; Kim, S. H.; Lin, S.; Bhattacharya, P.; Ke, P. C.; Lamm, M. H. *Phys. Chem. Chem. Phys.* **2010**, *12*, 9285.
(25) Solubility Table. http://en.wikipedia.org/wiki/Solubility_table.
(26) Karapanagioti, H. K. *Desalination* **2007**, *210*, 274.
(27) Barton, R. A.; Ilic, B.; Verbridge, S. S.; Cipriany, B. R.; Parpia, J. M.; Craighead, H. G. *Nano Lett.* **2010**, *10*, 2058.
(28) Mitra, A.; Deutsch, B.; Ignatovich, F.; Dykes, C.; Novotny, L. *ACS Nano* **2010**, *4*, 1305.
(29) Song, C.; Wang, P. *Appl. Phys. Lett.* **2009**, *94*, 023901.
(30) Yang, Y.; Zhang, H.; Zhu, J.; Wang, G.; Tzeng, T. R.; Xuan, X.; Huang, K.; Wang, P. *Lab Chip* **2010**, *10*, 553.
(31) Yeo, L. Y.; Chang, H.−C.; Chan, P. P. Y.; Friend, J. R. *Small* **2011**, *7*, 12.
(32) Taki, M.; Iyoshi, S.; Ojida, A.; Hamachi, I.; Yamamoto, Y. *J. Am. Chem. Soc.* **2010**, *132*, 5938.
(33) *The Merck Veterinary Manual*. Nitrate and Nitrite Poisoning: Introduction. http://www.merckvetmanual.com/mvm/index.jsp?cfile=htm/bc/212300.htm.
(34) U. S. Environmental Protection Agency. http://www.epa.gov/osw/hazard/wastemin/minimize/factshts/phenanth.pdf.
(35) U. S. Environmental Protection Agency. http://water.epa.gov/drink/contaminants/#List.
(36) Huissmann, S.; Wynveen, A.; Likos, C. N.; Blaak, R. *J. Phys.: Condens. Matter* **2010**, *22*, 232101.
(37) Crooks, R. M.; Zhao, M.; Sun, L.; Chechik, V.; Yeung, L. K. *Acc. Chem. Res.* **2001**, *34*, 181.
(38) Ottaviani, M. F.; Montalti, F.; Turro, N. J.; Tomalia, D. A. *J. Phys. Chem. B.* **1997**, *101*, 158.
(39) Zhao, M.; Crooks, R. M. *Adv. Mater.* **1999**, *11*, 217.
(40) Zhao, M.; Sun, L.; Crooks, R. M. *J. Am. Chem. Soc.* **1998**, *120*, 4877.
(41) Tomisic, V.; Simeon, V. *Phys. Chem. Chem. Phys.* **1999**, *1*, 299.
(42) Butorac, V.; Simeon, V.; Tomisic, V. *Croat. Chem. Acta.* **2007**, *80*, 533.